

Alma Mater Studiorum Università di Bologna  
Archivio istituzionale della ricerca

Propargyl carbamate-functionalized Cu(II)-metal organic framework after reaction with chloroauric acid: An x-ray photoelectron spectroscopy data record

This is the final peer-reviewed author's accepted manuscript (postprint) of the following publication:

*Published Version:*

Pagot, G., Cassani, M.C., Gambassi, F., Ballarin, B., Nanni, D., Coi, M., et al. (2022). Propargyl carbamate-functionalized Cu(II)-metal organic framework after reaction with chloroauric acid: An x-ray photoelectron spectroscopy data record. SURFACE SCIENCE SPECTRA, 29, 1-10 [10.1116/6.0001950].

*Availability:*

This version is available at: <https://hdl.handle.net/11585/897296> since: 2022-10-26

*Published:*

DOI: <http://doi.org/10.1116/6.0001950>

*Terms of use:*

Some rights reserved. The terms and conditions for the reuse of this version of the manuscript are specified in the publishing policy. For all terms of use and more information see the publisher's website.

This item was downloaded from IRIS Università di Bologna (<https://cris.unibo.it/>).  
When citing, please refer to the published version.

(Article begins on next page)

This is the final peer-reviewed accepted manuscript of:

**Pagot, G.; Cassani, M. C.; Gambassi, F.; Ballarin, B.; Nanni, D.; Coi, M.; Barreca, D.; Boanini, E.; Di Noto, V. Propargyl Carbamate-Functionalized Cu(II)-Metal Organic Framework after Reaction with Chloroauric Acid: An x-Ray Photoelectron Spectroscopy Data Record. Surface Science Spectra 2022, 29 (2), 024007**

The final published version is available online at: <https://doi.org/10.1116/6.0001950>

#### Terms of use:

Some rights reserved. The terms and conditions for the reuse of this version of the manuscript are specified in the publishing policy. For all terms of use and more information see the publisher's website.

*This item was downloaded from IRIS Università di Bologna (<https://cris.unibo.it/>)*

***When citing, please refer to the published version.***

# Propargyl carbamate-functionalized Cu(II)-MOF after reaction with chloroauric acid: an XPS data record

Gioele Pagot,<sup>1,2</sup> Maria Cristina Cassani,<sup>3,a</sup> Francesca Gambassi,<sup>3</sup> Barbara Ballarin,<sup>3</sup> Daniele Nanni,<sup>3</sup> Michele Coi,<sup>3</sup> Davide Barreca,<sup>4</sup> Elisa Boanini,<sup>5</sup> Vito Di Noto<sup>1,2,a</sup>

<sup>1</sup> Section of Chemistry for the Technology (ChemTech), Dept. of Industrial Engineering, University of Padova, Via Marzolo 9, I-35131 Padova (PD), Italy

<sup>2</sup> INSTM - Section at the Dept. of Industrial Engineering, University of Padova, Via Marzolo 9, I-35131 Padova (PD), Italy

<sup>3</sup> Dept. of Industrial Chemistry "Toso Montanari", Bologna University, Viale Risorgimento 4, I-40136, Bologna, Italy

<sup>4</sup> CNR-ICMATE and INSTM, Dept. of Chemical Sciences, Padova University, Via Marzolo 1, I-35131, Padova, Italy

<sup>5</sup> Dept. of Chemistry "Giacomo Ciamician", Bologna University, Via Selmi 2, I-40126, Bologna, Italy

(Received day Month year; accepted day Month year; published day Month year)

A copper-containing metal organic framework (MOF) was prepared using the new organic linker 5-(2-((prop-2-yn-1-yloxy)carbonyl)-amino)ethoxy)isophthalic acid (1,3-H<sub>2</sub>YBDC (where Y = alkYne and BDC = Benzene DiCarboxylate), and functionalized with gold particles by reaction with HAuCl<sub>4</sub> under thermal treatment in methanol. The resulting system was investigated by complementary techniques to obtain information on structure and morphology. In the present work, X-ray photoelectron spectroscopy (XPS) was employed to analyse the chemical composition of a representative specimen. Beside wide scan spectra, data obtained by the analysis of the C1s, O1s, N1s, Cu2p and Au4f signals are presented and critically discussed. The results highlight the reduction of Au(III) to Au(0) and to Au(I), with the latter oxidation state being the predominant one. Overall, the data presented herein may act as useful guidelines for the eventual tailoring of material properties and their possible implementation towards functional applications in heterogeneous catalysis.

**Keywords:** Metal organic framework, copper, benzene dicarboxylate, propargyl carbamate, gold, X-ray photoelectron spectroscopy

## INTRODUCTION

Metal-Organic Frameworks (MOFs) constituted by connecting metal ions with polytopic organic linkers have received enormous attention in the last decade. Their tuneable pore geometries and flexible frameworks have been successfully exploited in various research fields such as catalysis, gas absorption, gas storage or sensing (Refs. 1-9).

In recent years, our research group has shown that a propargyl carbamate [-N(H)C(O)O-CH<sub>2</sub>-C≡CH] group anchored on different oxide supports (SiO<sub>2</sub>, Al<sub>2</sub>O<sub>3</sub>, TiO<sub>2</sub>, Fe<sub>3</sub>O<sub>4</sub>) is capable of reducing Au(III) to Au(0), yielding supported gold nanoparticles (AuNPs) without the addition of any external reducing and/or stabilizing agent (Refs. 10-13). Based on these results and considering that the chemical, structural, and functional behaviour of AuNPs are directly dependent on the physico-chemical environment dictated by the support, we envisaged that

the versatility demonstrated by the propargyl carbamate residue could be further exploited by anchoring it to solid supports different from oxides, for example within alkynyl-derivatized MOFs. In this regard, we showed that the reaction of the novel 5-substituted organic linker 5-(2-((prop-2-yn-1-yloxy)carbonyl)-amino)ethoxy)isophthalic acid (labelled 1,3-H<sub>2</sub>YBDC, where Y = alkYne and BDC = Benzene DiCarboxylate), bearing a propargyl carbamate substituent, with copper nitrate in refluxing 2-propanol leads to a new copper-based MOF Cu-YBDC in high yields. The novel material was fully characterized by complementary analytical techniques. X-ray diffraction (XRD) data revealed that Cu-YBDC contains a complex network of 5-substituted isophthalate anions coordinated to Cu(II) centers belonging to the common paddlewheel dimeric structure with a Cu-Cu distance of 2.633 Å. Quite unexpectedly, the apical atom in the paddlewheel structure belongs to the carbonyl atom of the propargyl carbamate functionality, present with two equally

---

**Accession#:** Enter  
Accession Number.

**Technique:** XPS

**Host Material:** [Cu(1,3-YBDC)]·(C<sub>14</sub>H<sub>11</sub>NO<sub>8</sub>Cu) and Au

**Instrument:** Perkin-Elmer  
Physical Electronics, Inc.  
5600ci

**Major Elements in Spectra:** C, O, N, Cu

**Minor Elements in Spectra:** Au

**Published Spectra:** 6

**Spectra in Electronic Record:** 8

**Spectral Category:**  
comparison

---

<sup>a</sup>Electronic mail: maria.cassani@unibo.it; vito.dinoto@unipd.it

populated alternative chain conformations. Such extra-coordination by the propargyl carbamate groups drastically reduces the MOF porosity, as also confirmed by BET measurements. Despite this evidence suggests that the internal material pores are available only to a small extent to host reactive gold species, this system stands as an attractive candidate for the generation and anchoring of reduced gold species on the MOF surface. This capability can be, in turn, related to its uniform array of propargyl-carbamate residues branching out therefrom and acting as binding sites able to capture Au(III) ions and subsequently forming Au(0) clusters (Refs. 14-15).

In this context, the present study focuses on the reactivity of Cu-YBDC with H<sub>2</sub>AuCl<sub>4</sub> under thermal treatment in refluxing methanol. The structure, morphology, and chemical composition of the developed system has been analysed by means of atomic absorption spectroscopy (AAS), thermogravimetric analysis (TGA), XRD, field emission scanning electron microscopy (FE-SEM). X-ray photoelectron spectroscopy (XPS) studies were performed on a selected representative sample using a standard AlK $\alpha$  X-ray excitation source. This investigation was carried out in order to gather information on the elemental composition, oxidation states and chemical environments characterizing the elements present in the investigated material.

#### **SPECIMEN DESCRIPTION (ACCESSION # FG82.)**

**Host Material:** [Cu(1,3-YBDC)] $\cdot$ (C<sub>14</sub>H<sub>11</sub>NO<sub>8</sub>Cu) and Au

**CAS Registry #:** unknown

**Host Material Characteristics:** homogeneous; solid; polycrystalline; unknown conductivity; Powder

**Chemical Name:** [Cu(1,3-YBDC)] $\cdot$ (C<sub>14</sub>H<sub>11</sub>NO<sub>8</sub>Cu) and Au

**Source:** In a 100 mL round-bottom flask, a suspension of 1,3-H<sub>2</sub>YBDC (0.120 g, 0.390 mmol) and Cu(NO<sub>3</sub>)<sub>2</sub> $\cdot$ 2.5H<sub>2</sub>O (0.163 g, 0.701 mmol) in 2-propanol (15 mL) was refluxed at 83 °C under stirring (300 rpm) for 24 h and then cooled down to room temperature. The precipitate was collected by Buchner filtration and washed with 2-propanol (2 $\times$ 10 mL). The turquoise microcrystalline powder was subsequently dried in an oven at 70 °C for 24 h, subsequently kept under vacuum (0.02 bar) for 24 h and stored under nitrogen to give 0.142 g of [Cu(1,3-YBDC)] $\cdot$ xH<sub>2</sub>O (yield = 90% based on the organic acid and considering the Cu-MOF dihydrate).

**Host Composition:** C, H, N, O, Cu and Au

**Form:** powder

**Structure:** The system structure was investigated by complementary techniques (AAS, TGA, XRD, FE-SEM) and the resulting data compared with the pristine Cu-MOF. The amount of adsorbed gold by was 0.8 wt.%. The TGA plot for the Au-containing Cu-MOF showed that, similarly to the starting Cu-MOF, two decomposition steps occur in the range 200-450 °C range with a final residue of  $\approx$  30 wt%, *i.e.*, a 4 wt% higher than in the absence of gold. XRD patterns of Cu-YBDC and Cu-MOF/Au are identical, except for the fact that in Cu-MOF/Au the peak at 12.82° (attributed to Cu<sub>2</sub>(OH)<sub>3</sub>(NO<sub>3</sub>) contaminating species) is more intense. FE-SEM images of Cu-YBDC/Au (see

the inset in figure Accession # FG82-01) revealed the predominant presence of prismatic aggregates.

**History & Significance:** H<sub>2</sub>AuCl<sub>4</sub> $\times$ 3H<sub>2</sub>O (0.050 g, 0.127 mmol) was added to a suspension of Cu-YBDC (0.250 g) in MeOH (120 mL). The reaction mixture was stirred for 1 h at room temperature, and the solid was subsequently separated from the supernatant by centrifugation at 5400 rpm for 15 min. After three cycles of washing with MeOH (3 $\times$ 20 mL) and centrifugation, the product was stirred in MeOH (30 mL) at 65°C for 1 h. The solid was again separated by centrifugation and washed with MeOH.

**As Received Condition:** As grown.

**Analyzed Region:** Same as host material

**Ex Situ Preparation/Mounting:** Sample fixed on an adhesive tape and directly introduced into the analysis chamber through a fast entry.

**In Situ Preparation:** None

**Charge Control:** No flood gun was used during analysis. For further details on the charging correction procedure, see Data Analysis Methods, Energy Scale Correction.

**Temp. During Analysis:** 298 K

**Pressure During Analysis:** <10<sup>-4</sup> Pa

**Pre-analysis Beam Exposure:** 180 s.

#### **INSTRUMENT DESCRIPTION**

**Manufacturer and Model:** Perkin-Elmer Physical Electronics, Inc. 5600ci

**Analyzer Type:** spherical sector

**Detector:** Channeltron

**Number of Detector Elements:** 16

#### **INSTRUMENT PARAMETERS COMMON TO ALL SPECTRA**

##### **■ Spectrometer**

**Analyzer Mode:** constant pass energy

**Throughput (T=E<sup>N</sup>):** N=0

**Excitation Source Window:** 1.5 micron Al window

**Excitation Source:** Al K $\alpha$

**Source Energy:** 1486.6 eV

**Source Strength:** 200 W

**Source Beam Size:** > 25000  $\mu$ m x > 25000  $\mu$ m

**Signal Mode:** multichannel direct

##### **■ Geometry**

**Incident Angle:** 9 °

**Source-to-Analyzer Angle:** 53.8 °

**Emission Angle:** 45 °

**Specimen Azimuthal Angle:** 0 °

**Acceptance Angle from Analyzer Axis:** 0 °

**Analyzer Angular Acceptance Width:** 14°  $\times$  14°

## ■ Ion Gun

**Manufacturer and Model:** PHI 04-303 A

**Energy:** 4000 eV

**Current:** 0.4 mA/cm<sup>2</sup>

**Current Measurement Method:** Faraday cup

**Sputtering Species:** Ar<sup>+</sup>

**Spot Size (unrastered):** 250 μm

**Raster Size:** 2000 μm x 2000 μm

**Incident Angle:** 40 °

**Polar Angle:** 45 °

**Azimuthal Angle:** 111 °

**Comment:** differentially pumped ion gun

## DATA ANALYSIS METHOD

**Energy Scale Correction:** Binding energy (BE) values were corrected for charging by assigning to the adventitious C1s peak a BE of 284.8 eV (Ref. 16).

**Recommended Energy Scale Shift:** -2.4 eV.

**Peak Shape and Background Method:** Gaussian-Lorentzian functions were used for peak fitting, with a typical composition value of ~80 % Gaussian and ~20 % Lorentzian. No G/L constraints were applied during the fitting. A Shirley background function was used.

**Quantitation Method:** Atomic concentrations were calculated by peak area integration, using sensitivity factors provided by PHI V5.4A software.

## ACKNOWLEDGMENTS

Bologna University, CNR (Progetti di Ricerca @CNR – avviso 2020 – ASSIST), and INSTM Consortium (INSTM21PDBARMAC - ATENA) are gratefully acknowledged for financial support. G.P. and V.D.N. gratefully acknowledge Padova University for support *via* the program “Budget Integrato per la Ricerca Interdipartimentale - BIRD 2021”, project number BIRD219831.

## AVAILABILITY OF DATA

The data that supports the findings of this study are available within the article and its supplementary material.

## CONFLICT OF INTEREST

The authors have no conflicts to disclose.

## REFERENCES

- <sup>1</sup>X.-H. Bu, M.J. Zaworotko, and Z. Zhang, *Metal-Organic Framework: From Design to Applications*, 1<sup>st</sup> ed. (Springer, Switzerland, 2020), pp. 1-426.
- <sup>2</sup>A.J. Howarth, A.W. Peters, N.A. Vermeulen, T.C. Wang, J.T. Hupp, and O.K. Farha, *Chem. Mater.* **29**, 26 (2017).
- <sup>3</sup>N. Stock, and S. Biswas, *Chem. Rev.* **112**, 933 (2012).
- <sup>4</sup>A.H. Chughtai, N. Ahmad, H.A. Younus, A. Laypkov, and F. Verpoort, *Chem. Soc. Rev.* **44**, 6804 (2015).
- <sup>5</sup>Q. Wang, and D. Astruc, *Chem. Rev.* **120**, 1438 (2020).
- <sup>6</sup>F.G. Cirujano, N. Martin, and L.H. Wee, *Chem. Mater.* **32**, 10268 (2020).

- <sup>7</sup>M. Ding, R.W. Flaig, H.-L. Jiang, and O.M. Yaghi, *Chem. Soc. Rev.* **48**, 2783 (2019).
- <sup>8</sup>M.D. Allendorf, and V. Stavila, *CrystEngComm* **17**, 229 (2015).
- <sup>9</sup>M. Köberl, M. Cokoja, W.A. Herrmann, and F.E. Kühn, *Dalton Trans.* **40**, 6834 (2011).
- <sup>10</sup>S. Fazzini, M.C. Cassani, B. Ballarin, E. Boanini, J.S. Girardon, A.-S. Mamede, A. Mignani, and D. Nanni, *J. Phys. Chem. C* **118**, 24538 (2014).
- <sup>11</sup>B. Ballarin, M.C. Cassani, D. Nanni, C. Parise, D. Barreca, G. Carraro, A. Riminucci, I. Bergenti, V. Morandi, A. Migliori, and E. Boanini, *Ceram. Int.* **45**, 449 (2019).
- <sup>12</sup>C. Parise, B. Ballarin, D. Barreca, M.C. Cassani, P. Dambruoso, D. Nanni, I. Ragazzini, and E. Boanini, *Appl. Surf. Sci.* **492**, 45 (2019).
- <sup>13</sup>B. Ballarin, D. Barreca, E. Boanini, M.C. Cassani, P. Dambruoso, A. Massi, A. Mignani, D. Nanni, C. Parise, and A. Zaghi, *ACS Sustain. Chem. Eng.* **5**, 4746 (2017).
- <sup>14</sup>M.C. Cassani, F. Gambassi, B. Ballarin, D. Nanni, I. Ragazzini, D. Barreca, C. Maccato, A. Guagliardi, N. Masciocchi, A. Kovtun, K. Rubini, and E. Boanini, *RSC Adv.* **11**, 20429 (2021).
- <sup>15</sup>M.C. Cassani, R. Castagnoli, F. Gambassi, D. Nanni, I. Ragazzini, N. Masciocchi, E. Boanini, and B. Ballarin, *Sensors* **21**, 4922 (2021).
- <sup>16</sup>D. Briggs, and M.P. Seah, *Practical surface analysis: Auger and X-ray photoelectron spectroscopy*, 2<sup>nd</sup> ed. (John Wiley & Sons, New York, 1990), pp. 1-657.
- <sup>17</sup>M.R. Azhar, G. Hussain, M.O. Tade, D.S. Silvester, and S. Wang, *ACS Appl. Nano Mater.* **3**, 4376 (2020).
- <sup>18</sup>J.F. Moulder, W.F. Stickle, P.E. Sobol, and K.D. Bomben, *Handbook of X-ray Photoelectron Spectroscopy*, 1<sup>st</sup> ed. (Perkin Elmer Corporation, Eden Prairie, MN, USA, 1992), pp. 1-261.
- <sup>19</sup><http://srdata.nist.gov/xps>.
- <sup>20</sup>J. Li, T. Zhao, M. M. Shirolkar, M. Li, H. Wang, and H. Li, *Nanomaterials* **9**, 790 (2019).
- <sup>21</sup>X. Li, J. Wan, Y. Ma, J.R. Zhao, and Y. Wang, *Appl. Surf. Sci.* **510**, 145459 (2020).
- <sup>22</sup>X. Zhao, W. Wu, G. Jing, and Z. Zhou, *Environ. Pollut.* **260**, 114038 (2020).
- <sup>23</sup>A. Taher, D.W. Kim, and I.-M. Lee, *RSC Adv.* **7**, 17806 (2017).
- <sup>24</sup>D. Barreca, G. Carraro, and A. Gasparotto, *Surf. Sci. Spectra* **16**, 1 (2009).
- <sup>25</sup>R. Senthil Kumar, S. Senthil Kumar, and M. Anbu Kulandainathan, *Microporous Mesoporous Mater.* **168**, 57 (2013).
- <sup>26</sup>D. Barreca, A. Gasparotto, C. Maccato, E. Tondello, O.I. Lebedev, and G. Van Tendeloo, *Cryst. Growth Des.* **9**, 2470 (2009).
- <sup>27</sup>C. Chen, T. Wu, D. Yang, P. Zhang, H. Liu, Y. Yang, G. Yang, and B. Han, *Chem. Comm.* **54**, 5984 (2018).

SPECTRAL FEATURES TABLE							
Spectrum ID #	Element/Transition	Peak Energy (eV)	Peak Width FWHM (eV)	Peak Area (eV x cts/s)	Sensitivity Factor	Concentration (at. %)	Peak Assignment
FG82-02 <sup>a</sup>	C 1s	284.8	2.1	12730.2	0.296	28.3	Aliphatic carbon arising from adventitious surface contamination
FG82-02 <sup>a</sup>	C 1s	286.2	2.2	9099.5	0.296	20.2	C-N and C-O bonds in the ligand skeleton
FG82-02 <sup>a</sup>	C 1s	288.1	1.9	2893.6	0.296	6.4	-COOH functionalities bonded to the aromatic ring
FG82-02 <sup>a</sup>	C 1s	289.5	2.1	3771.2	0.296	8.4	-NCOO- groups present in the ligand lateral chain
FG82-03 <sup>b</sup>	O 1s	530.2	1.8	2941.3	0.711	2.6	ligand oxygen atoms bonded to copper and O in Cu <sub>2</sub> (OH) <sub>3</sub> (NO <sub>3</sub> )
FG82-03 <sup>b</sup>	O 1s	531.9	1.8	10814.81	0.711	9.7	C-O single bonds, chemisorbed hydroxyl groups and OH groups in Cu <sub>2</sub> (OH) <sub>3</sub> (NO <sub>3</sub> )
FG82-03 <sup>b</sup>	O 1s	533.3	2.6	18298.2	0.711	16.4	C=O groups in carboxylate functionalities and/or adsorbed water molecules
FG82-04	N 1s	400.4	2.6	2810.7	0.477	3.7	Cu...N coordination
FG82-05 <sup>c</sup>	Cu 2p				5.321	0.9 <sup>d</sup>	Cu(I) species
FG82-05	Cu 2p <sub>3/2</sub>	932.8	2.4	2380.0			Cu(I) species
FG82-05	Cu 2p <sub>1/2</sub>	952.6	2.4	1262.3			Cu(I) species
FG82-05 <sup>c</sup>	Cu 2p				5.321	2.4 <sup>e</sup>	Cu(II) species
FG82-05	Cu 2p <sub>3/2</sub>	934.8	2.7	6189.8			Cu(II) species
FG82-05	Cu 2p <sub>1/2</sub>	954.6	3.1	2524.6			Cu(II) species
FG82-06 <sup>f</sup>	Au 4f				6.250	0.2 <sup>g</sup>	Au(0)
FG82-06	Au 4f <sub>7/2</sub>	84.0	1.8	988.9			Au(0)
FG82-06	Au 4f <sub>5/2</sub>	87.6	1.8	741.7			Au(0)
FG82-06 <sup>f</sup>	Au 4f				6.250	0.5 <sup>h</sup>	Au(I)
FG82-06	Au 4f <sub>7/2</sub>	85.3	1.7	2159.1			Au(I)
FG82-06	Au 4f <sub>5/2</sub>	88.9	1.7	1619.2			Au(I)
FG82-06 <sup>f</sup>	Au 4f				6.250	0.3 <sup>i</sup>	Au(III)
FG82-06	Au 4f <sub>7/2</sub>	86.4	1.8	1537.5			Au(III)
FG82-06	Au 4f <sub>5/2</sub>	90.0	1.8	1153.1			Au(III)
	Cu LMM	915.0 <sup>j</sup>					Cu species

<sup>a</sup>The sensitivity factor is referred to the whole C 1s signal.

<sup>b</sup>The sensitivity factor is referred to the whole O 1s signal.

<sup>c</sup>The sensitivity factor is referred to the whole Cu 2p signal.

<sup>d</sup>The atomic percentage is referred to the sole Cu(I) species.

<sup>e</sup>The atomic percentage is referred to the sole Cu(II) species.

<sup>f</sup>The sensitivity factor is referred to the whole Au4f signal.

<sup>g</sup>The atomic percentage is referred to the sole Au(0) species.

<sup>h</sup>The atomic percentage is referred to the only Au(I) species.

<sup>i</sup>The atomic percentage is referred to the only Au(III) species.

<sup>j</sup>The peak position is given in KE.

**Footnote to Spectrum FG82-02:** High-resolution C1s spectra reveal the presence of different components: BE = 284.8 eV ( $\approx$  45 % of the total C signal), attributed to aliphatic carbon arising from adventitious surface contamination; BE = 286.2 eV ( $\approx$  32 % of the total C), assigned to C-N and C-O bonds in the ligand skeleton; BE = 288.1 eV ( $\approx$  10 % of the total C signal), related to -COOH functionalities bonded to the aromatic ring; and BE = 289.5 eV ( $\approx$  13 % of the total C signal), assigned to -NCOO- groups present in the ligand lateral chain (Refs. 17-19).

**Footnote to Spectrum FG82-03:** Three different peaks are concurring to the overall intensity of the O1s signal,: BE = 530.2 eV ( $\approx$  9 % of the total O signal), associated to ligand oxygen atoms bonded to copper (Ref. 17) and O in Cu<sub>2</sub>(OH)<sub>3</sub>(NO<sub>3</sub>) (Ref. 20); BE = 531.9 eV ( $\approx$  34 % of the total O signal), ascribed to C-O single bonds, chemisorbed OH hydroxyl groups and OH groups in Cu<sub>2</sub>(OH)<sub>3</sub>(NO<sub>3</sub>) (Refs. 18, 20-22); and BE = 533.3 eV ( $\approx$  57 % of the total O signal), attributed to the presence of C=O groups in carboxylate functionalities and/or adsorbed water molecules (Refs. 18-19). The broadening of this latter peak is due to the presence of water molecules in slightly different surface environments.

**Footnote to Spectrum FG82-04:** A single peak signal is determined in the N1s spectra, centered at BE = 400.4 eV. This binding energy value indicates a strong ligand coordination between nitrogen atoms and copper metal centers in the investigated material (Ref. 23).

**Footnote to Spectrum FG82-05:** Information on the Cu chemical state can be gained by a careful evaluation of the copper signal. As performed in Ref. 24, both Cu2p<sub>3/2</sub> and Cu2p<sub>1/2</sub> peaks can be fitted with two components. The features at BE values of 932.8 and 952.6 eV are attributed to Cu2p<sub>3/2</sub> and Cu2p<sub>1/2</sub> spin-orbit components of Cu(I) species, while those peaking at 934.8 and 954.6 eV are related to Cu(II) species into the copper-containing metal-organic framework (Refs. 17, 22, 25). Peak analysis indicates that Cu(II) are the dominant species (*i.e.*, more than 70 % of the overall copper). A further confirmation of this attribution is given by the presence of intense *shake-up* satellites peaking at BE values  $\approx$  9.5 eV higher than the main spin-orbit components, which are a finger-print for the predominant presence of *d*<sup>9</sup> copper (II) centers (Refs. 24, 26-27). When only Cu(I) species (*d*<sup>10</sup>, a closed-shell system) are present, such satellites are not detected (Refs. 16, 23). The evaluation of the Auger parameter, defined as  $\alpha_{Cu} = BE(Cu2p_{3/2}) + KE(CuLMM)$  (Ref. 16) (where KE = kinetic energy), yielded a value of 1850.0 eV, intermediate between those reported for Cu(I) and Cu(II) species (Ref. 26).

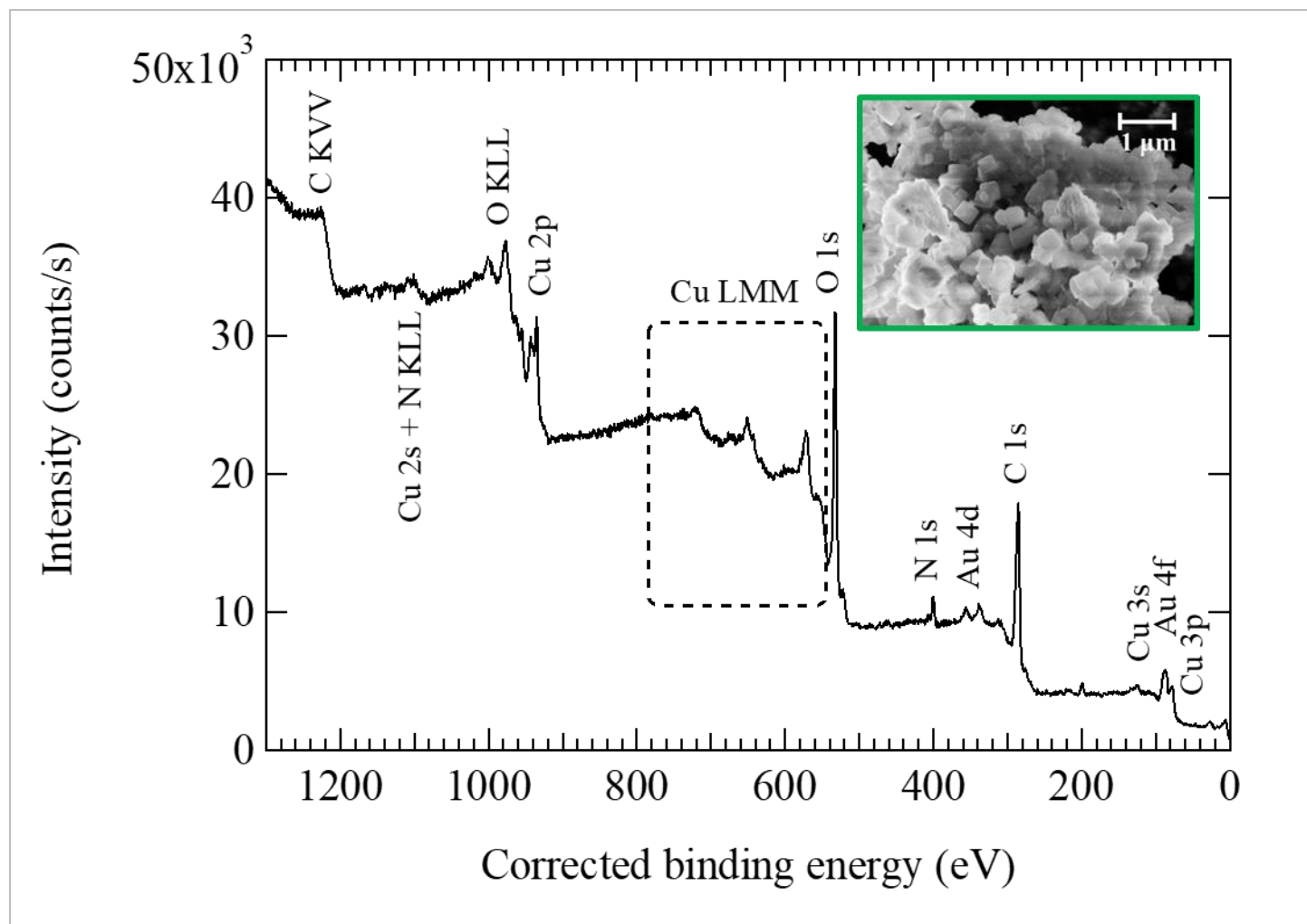
**Footnote to Spectrum FG82-06:** The fitting of the Au 4f peak enabled to recognize the co-presence of: (i) Au(0) species ( $BE(Au4f_{7/2}) = 84.0$  eV and  $BE(Au4f_{5/2}) = 87.6$  eV,  $\approx 21$  % of the total Au4f signal) (Refs. 13, 18); (ii) Au(I) species ( $BE(Au4f_{7/2}) = 85.3$  eV and  $BE(Au4f_{5/2}) = 88.9$  eV,  $\approx 46$  % of the total Au4f signal) (Refs. 16, 18-19); and (iii) Au(III) species ( $BE(Au4f_{7/2}) = 86.4$  eV and  $BE(Au4f_{5/2}) = 90.0$  eV,  $\approx 33$  % of the total Au4f signal) (Refs. 16, 18-19).

ANALYZER CALIBRATION TABLE							
Spectrum ID #	Element/ Transition	Peak Energy (eV)	Peak Width FWHM (eV)	Peak Area (eV x cts/s)	Sensitivity Factor	Concentration (at. %)	Peak Assignment
figCalib01 <sup>a</sup>	Au4f <sub>7/2</sub>	84.0	1.4	186403	...	...	Au(0)
figCalib02 <sup>a</sup>	Cu2p <sub>3/2</sub>	932.7	1.6	86973	...	...	Cu(0)

<sup>a</sup>The peak was acquired after Ar<sup>+</sup> erosion.

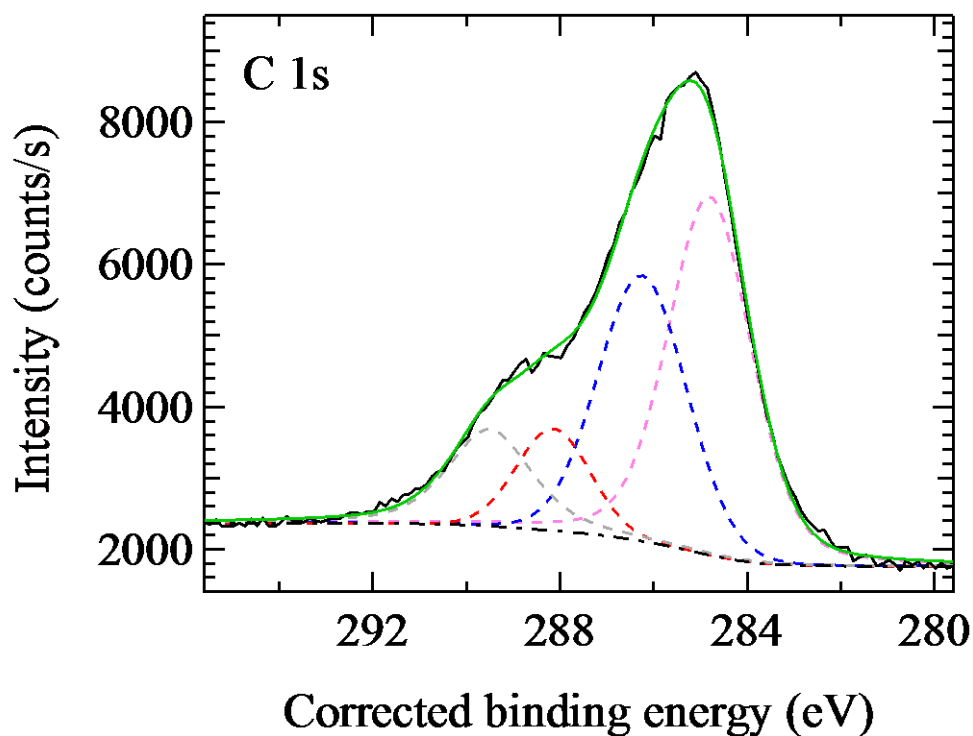
GUIDE TO FIGURES					
Spectrum (Accession) #	Spectral Region	Voltage Shift*	Multiplier	Baseline	Comment #
FG82-01	Survey	+2.4	1	0	...
FG82-02	C 1s	+2.4	1	0	...
FG82-03	O 1s	+2.4	1	0	...
FG82-04	N 1s	+2.4	1	0	...
FG82-05	Cu 2p	+2.4	1	0	...
FG82-06	Au 4f	+2.4	1	0	...

\*Voltage shift of the archived (as measured) spectrum relative to the printed figure.



Publish in *Surface Science Spectra*: Yes ☒ No ☐

Accession #	FG82-01
Host Material	[Cu(1,3-YBDC)]·(C <sub>14</sub> H <sub>11</sub> NO <sub>8</sub> Cu) and Au
Technique	XPS
Spectral Region	survey
Instrument	Perkin-Elmer Physical Electronics, Inc. 5600ci
Excitation Source	Al Ka
Source Energy	1486.6 eV
Source Strength	200 W
Source Size	> 25 mm x > 25 mm
Analyzer Type	spherical sector analyzer
Incident Angle	9°
Emission Angle	45°
Analyzer Pass Energy	187.85 eV
Analyzer Resolution	1.9 eV
Total Signal Accumulation Time	975.6 s
Total Elapsed Time	1073.2 s
Number of Scans	30
Effective Detector Width	1.9 eV



Publish in SSS: Yes ☒ No ☐

■ Accession #: FG82-02

■ Host Material: [Cu(1,3-YBDC)]-(C<sub>14</sub>H<sub>11</sub>NO<sub>8</sub>Cu) and Au

■ Technique: XPS

■ Spectral Region: C 1s

Instrument: Perkin-Elmer Physical Electronics, Inc. 5600ci

Excitation Source: Al Ka

Source Energy: 1486.6 eV

Source Strength: 200 W

Source Size: >25 mm x >25 mm

Analyzer Type: spherical sector

Incident Angle: 9 °

Emission Angle: 45 °

Analyzer Pass Energy 58.7 eV

Analyzer Resolution: 0.6 eV

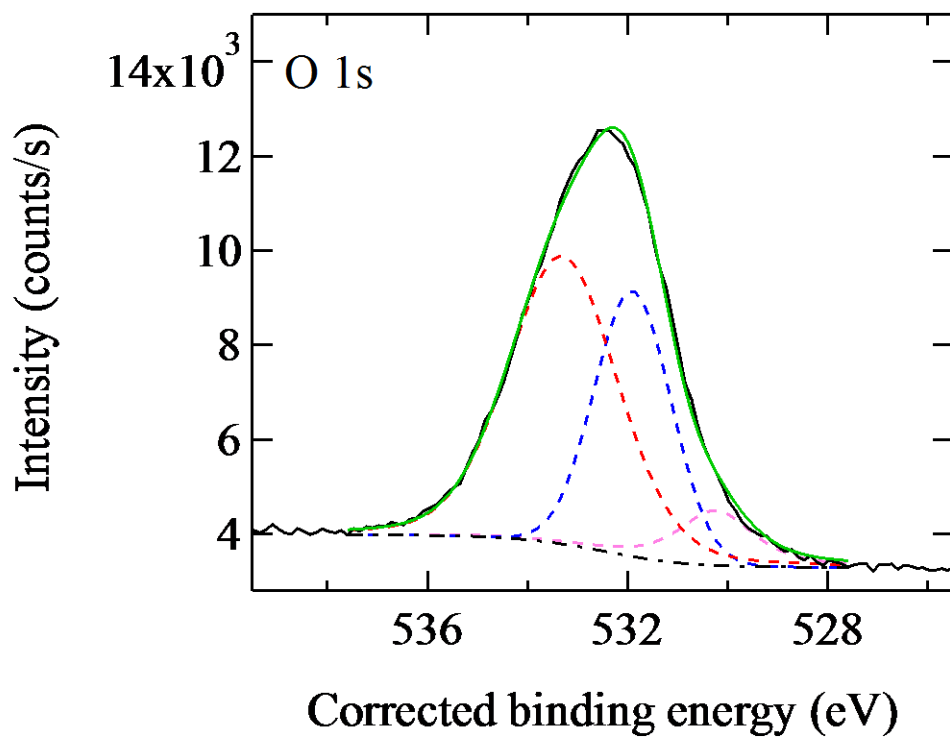
Total Signal Accumulation Time: 144.9 s

Total Elapsed Time: 159.4 s

Number of Scans: 18

Enter source energy.

Effective Detector Width: 0.6 eV



Publish in SSS: Yes ☒ No ☐

■ Accession #: FG82-03

■ Host Material: [Cu(1,3-YBDC)]-(C<sub>14</sub>H<sub>11</sub>NO<sub>8</sub>Cu) and Au

■ Technique: XPS

■ Spectral Region: O 1s

Instrument: Perkin-Elmer Physical Electronics, Inc. 5600ci

Excitation Source: Al Ka

Source Energy: 1486.6 eV

Source Strength: 200 W

Source Size: >25 mm x >25 mm

Analyzer Type: spherical sector

Incident Angle: 9 °

Emission Angle: 45 °

Analyzer Pass Energy 58.7 eV

Analyzer Resolution: 0.6 eV

Total Signal Accumulation Time: 144.9 s

Total Elapsed Time: 159.4 s

Number of Scans: 18Enter source

Effective Detector Width: 0.6 eV

Publish in SSS: Yes ☒ No ☐

■ Accession #: FG82-04

■ Host Material: [Cu(1,3-YBDC)]·(C<sub>14</sub>H<sub>11</sub>NO<sub>8</sub>Cu) and Au

■ Technique: XPS

■ Spectral Region: N 1s

Instrument: Perkin-Elmer Physical Electronics, Inc. 5600ci

Excitation Source: Al Ka

Source Energy: 1486.6 eV

Source Strength: 200 W

Source Size: >25 mm x >25 mm

Analyzer Type: spherical sector

Incident Angle: 9 °

Emission Angle: 45 °

Analyzer Pass Energy 58.7 eV

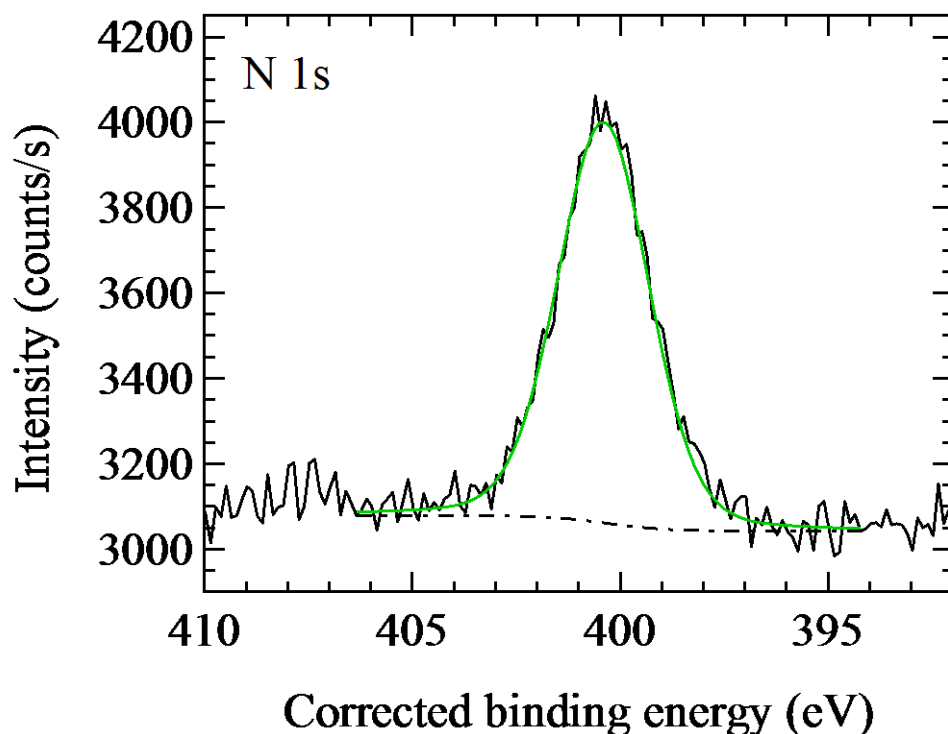
Analyzer Resolution: 0.6 eV

Total Signal Accumulation Time: 169.0 s

Total Elapsed Time: 185.9 s

Number of Scans: 21

Effective Detector Width: 0.6 eV



Publish in SSS: Yes ☒ No ☐

■ Accession #: FG82-05

■ Host Material: [Cu(1,3-YBDC)]·(C<sub>14</sub>H<sub>11</sub>NO<sub>8</sub>Cu) and Au

■ Technique: XPS

■ Spectral Region: Cu 2p

Instrument: Perkin-Elmer Physical Electronics, Inc. 5600ci

Excitation Source: Al Ka

Source Energy: 1486.6 eV

Source Strength: 200 W

Source Size: >25 mm x >25 mm

Analyzer Type: spherical sector

Incident Angle: 9 °

Emission Angle: 45 °

Analyzer Pass Energy 58.7 eV

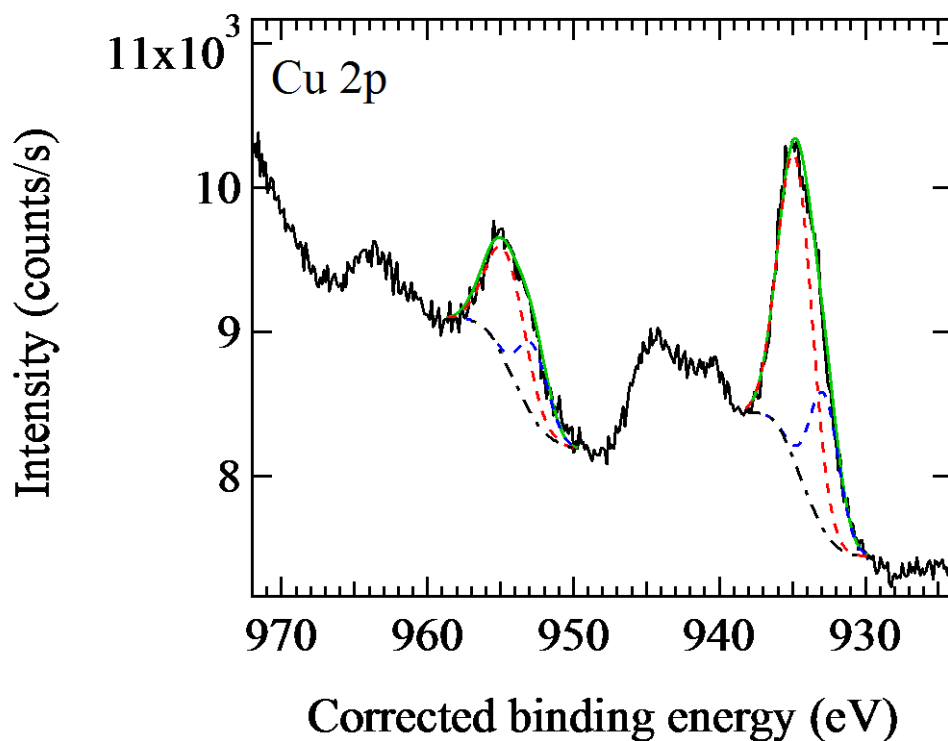
Analyzer Resolution: 0.6 eV

Total Signal Accumulation Time: 661.5 s

Total Elapsed Time: 727.7 s

Number of Scans: 30

Effective Detector Width: 0.6 eV



■ **Accession #:** FG82-06

■ **Host Material:** [Cu(1,3-YBDC)]·(C<sub>14</sub>H<sub>11</sub>NO<sub>8</sub>Cu) and Au

■ **Technique:** XPS

■ **Spectral Region:** Au 4f

Instrument: Perkin-Elmer Physical Electronics, Inc. 5600ci  
Excitation Source: Al Ka

Source Energy: 1486.6 eV

Source Strength: 200 W

Source Size: >25 mm x >25 mm

Analyzer Type: spherical sector

Incident Angle: 9 °

Emission Angle: 45 °

Analyzer Pass Energy 58.7 eV

Analyzer Resolution: 0.6 eV

Total Signal Accumulation Time:  
724.5 s

Total Elapsed Time: 797.0 s

Number of Scans: 90

Effective Detector Width: 0.6 eV

